



# Proton conducting polymer electrolyte based on cornstarch, PVP, and NH<sub>4</sub>Br for energy storage applications

M. Anandha Jothi<sup>1,2</sup> · D. Vanitha<sup>1,2</sup> · S. Asath Bahadur<sup>1,3</sup> · N. Nallamuthu<sup>1,2</sup>

Received: 20 April 2020 / Revised: 22 August 2020 / Accepted: 21 September 2020 / Published online: 2 November 2020  
© Springer-Verlag GmbH Germany, part of Springer Nature 2020

## Abstract

Proton conducting polymer blend electrolytes based on cornstarch and polyvinyl pyrrolidone (PVP) with ammonium bromide (NH<sub>4</sub>Br) were prepared by the technique of solution casting. Enhancement of amorphous nature by the addition of NH<sub>4</sub>Br has confirmed by XRD. In FTIR, by the addition of NH<sub>4</sub>Br salt in the optimized blend system, there occurs a change like altering the peak intensity, peak shape, and position. This reveals the appearance of complex formation between the polymer and salt. At 358 K, 30 wt.% of NH<sub>4</sub>Br added system shows the maximum conductivity ( $1.31 \times 10^{-4} \text{ S cm}^{-1}$ ). The conduction mechanism of higher conducting polymer blend electrolytes follows the quantum mechanical tunneling (QMT) at mid-frequency and overlapping large polaron tunneling (OLPT) at higher frequency. High dielectric constant and low relaxation time of ions in polymer chain are obtained for 30 wt.% of NH<sub>4</sub>Br added polymer blend electrolyte. From Wagner's polarization technique, it is established that conduction present in the polymer electrolytes is predominately due to ions. Faradaic pseudo capacity behaviour has observed in higher conducting sample by cyclic voltammetry. The electrochemical cell has prepared by the higher conducting polymer electrolyte and the open circuit potential (OCP) of 1.24 V has achieved from prepared electrochemical cell.

**Keywords** FTIR · Polymer electrolytes · Proton conductors · Electrochemical characterizations · Ionic conductivities

## Introduction

Recently, both academia and industrial researchers have focused great attention in the interdisciplinary field of polymer electrolytes which includes the discipline of polymer physics, electrochemistry, organic chemistry, and inorganic chemistry for the new electrochemical devices (batteries, super capacitors, fuel cells, solar cells, sensors, etc.). It has created revolutionize in many industrial areas [1–5]. Solid polymer electrolyte (SPE) has more advantages due to its excellent electrode

and electrolyte interface contact, no leakage problem, high safety, good mechanical, and adhesive properties [6–10]. In worldwide, the biodegradable polymers have enormous attention for avoiding environmental polluting chemicals. For recent researchers, there exists a great challenge to prepare a polymer electrolyte with good ionic conductivity, dimensional with mechanical stability, and low cost. Several characteristics are needed for selection of successful host polymer in SPE. These are environmental friendly, biocompatibility, biodegradable, abundant nature, solubility, donor groups (lone pair of electron) and less bond rotation barriers for the segmental motion [11, 12]. Biopolymers are suitable substitute for synthetic polymers because most of the synthetic polymers are insoluble in solvents and non-biodegradable material [1]. Many biopolymers as (starch, cornstarch, potato starch, pectin, amylose and polysaccharide) are easily available in nature. But the biopolymer cornstarch has a great attention due to its rich variety and abundance in nature. However, pure cornstarch film is brittle and rapidly degrades when exposed to water. PVP is also a biocompatible polymer used as blood plasma expander for trauma victims. PVP is an amorphous polymer possessing high  $T_g$  due to the presence of the rigid pyrrolidine group, which is known to form various complexes

✉ D. Vanitha  
vanibala2003@gmail.com

<sup>1</sup> Department of Physics, School of Advanced Science (SAS), Kalasalingam Academy of Research and Education, Krishnankoil, Srivilliputhur 626 126, India

<sup>2</sup> Multifunctional Materials Laboratory, International Research Centre, Kalasalingam Academy of Research and Education, Krishnankoil, Srivilliputhur 626 126, India

<sup>3</sup> Condensed Matter Physics Laboratory, International Research Centre, Kalasalingam Academy of Research and Education, Krishnankoil, Srivilliputhur 626 126, India

with many inorganic salts. PVP deserves a special attention among the conjugated polymers, because of its good environmental stability, easy process ability, and moderate electrical conductivity and it has broad range of applications such as electrochemical devices (batteries, displays). Based on these criteria, cornstarch and polyvinyl pyrrolidone (PVP) were selected as host polymers in the PEs. Ammonium salt and inorganic acids are  $H^+$  ion suppliers, for example, phosphoric acid ( $H_3PO_4$ ) and sulfuric acid ( $H_2SO_4$ ) based polymer electrolyte, which are described by encountering chemical degradation and poor mechanical integrity. In this manner, ammonium salts are the  $H^+$  ion suppliers that are used in polymer electrolytes because of their compatibility, high ionic conductivity and thermal stability [13, 14]. In the polymer-ammonium salt system, either  $NH_4^+$  or  $H^+$  plays a role in conduction, but many works have reported that the ionic conduction was due to the  $H^+$  in the system. The protons ( $H^+$ ) in polymer-ammonium complexes are covalently bound to the nitrogen, and consequently form hydrogen bonds with other electronegative atom [15–17]. Shukur and Kadir reported the ionic conductivity of  $(5.57 \pm 1.88) \times 10^{-5} S cm^{-1}$  for 70 wt.% starch–30 wt.%  $NH_4Br$  SPE [18]. So ammonium bromide ( $NH_4Br$ ) is chosen as a salt to polymer electrolyte for this work to improve the proton conductivity in the polymer blend electrolytes system.

## Materials and methods

### Materials for SPE preparation

Cornstarch ( $C_6H_{10}O_5$ )<sub>n</sub> and PVP ( $C_6H_9NO$ )<sub>n</sub> were acquired from SRL chemicals and SD Fine-Chem. Ltd., India, respectively. Ammonium bromide ( $NH_4Br$ ) was purchased from Avra Chem. Ltd. Acetic acid was procured from Reachem Laboratory Chemicals Private Limited, Chennai. In the whole synthesis of SPE films, double distilled water was used as a solvent.

### Materials for electrochemical cell preparation

Anode materials of Zn metal (powder) and  $ZnSO_4 \cdot 7H_2O$  were procured from SRL Chemicals (SISCO Research Laboratories Pvt. Ltd). Cathode material of  $MnO_2$  was obtained from Avra Chem. Ltd. Graphite was purchased from SD Fine-Chem. Ltd., India (SDFCL).

### Characterization techniques

Structural behaviour of prepared polymer electrolytes are characterized by X-Ray diffractometer made by Bruker Instruments having Cu-K $\alpha$  radiation ( $\lambda = 1.540 \text{ \AA}$ ) with scanning rate  $5^\circ$  per minute in the range of  $10^\circ$ – $60^\circ$ . The functional

group in the present polymer matrices is identified by SHIMADZU IR Tracer 100" Spectrometer with a resolution of  $4 cm^{-1}$ . Impedance analyses are carried out using HIOKI 3532-50 LCR Hi-tester within frequency range of 42 Hz–1 MHz in the temperature range of 303–358 K. The electrochemical property of prepared sample was investigated by using cyclic voltammetry on CH-Instrument Model 6008e.

### SPE preparation

80 wt.% cornstarch was dissolved in 50 ml of 1% acetic acid at 353 K for 20 min. After that solution was cooled down at room temperature under constant stirring for about 40 min. 20 wt.% PVP and different wt.%  $NH_4Br$  (5–35 wt.%) were separately dissolved in distilled water. These solutions were added one by one with 1 h delay to cornstarch solution. The solutions were mixed with a constant stirrer until occurring of consistent viscous solution. The last viscous solution was transformed into Petri dishes and it was allowed for evaporation of excess solvent traces in room temperature for 3 days. Then polymer film expelled from Petri dish for further analysis. Sample code assignment of different composition of the prepared polymer electrolytes are shown in Table 1.

### Electrochemical cell preparation

Under 2000 Pa hydraulic pressure for 5 min, 1 g of  $MnO_2$  (cathode) and 3:2 ratio of Zn metal (powder) and  $ZnSO_4 \cdot 7H_2O$  (anode) pellets were prepared separately. Finally, solid-state electrochemical cell was fabricated with the configuration of Graphite | Cathode | Higher conducting SPE | Anode | Graphite.

## Result and discussion

### X-ray diffraction

X-ray diffraction (XRD) pattern of prepared SPEs is displayed in Fig. 1a and b. Semi crystalline behaviour of cornstarch is

**Table 1** Sample code assignment for prepared polymer electrolytes

Composition ratio (cornstarch:PVP: $NH_4Br$ )	Sample code
80:20:0	CPN-0
80:20:5	CPN-5
80:20:10	CPN-10
80:20:15	CPN-15
80:20:20	CPN-20
80:20:25	CPN-25
80:20:30	CPN-30
80:20:35	CPN-35

confirmed by the presence of peaks at 16.9°, 19.5°, 21.9°, and medium sharp peak at 23.7° [19]. PVP does not have any distinguish peaks, because it is an amorphous polymer [20]. The intensity of the peaks is reduced to maximum for 80 wt.% cornstarch and 20 wt.% PVP added polymer blend system as shown in Fig. 1a. In Fig. 1b, the relative intensity of cornstarch peaks also significantly decreases by addition of NH<sub>4</sub>Br. This means addition of NH<sub>4</sub>Br salt modifies the ordered arrangement within the polymer membrane and reduces the crystalline nature of blend SPE. Also, there are no significant peaks of NH<sub>4</sub>Br for the samples from CPN-5 to CPN-30. This indicates that NH<sub>4</sub>Br is well associated to form the complexation to the polymer matrix [21]. For the sample CPN-30, there exists a suppression of hump which indicates the more amorphous nature. Further rising the salt concentration to the polymer matrix, two sharp peaks appeared at  $2\theta = 21.5^\circ$  and  $28.5^\circ$  corresponding to crystalline nature of NH<sub>4</sub>Br (JCPDS-85-0999).

### Fourier transform infrared spectroscopy

Fourier transform infrared (FTIR) is the potent tool to study about molecular interaction, variation of chemical bonding in polymer blend electrolytes on the addition of salt. Figure 2a shows the FTIR transmittance spectrum of cornstarch, PVP, and optimized cornstarch: PVP polymer electrolytes and Fig. 2b shows the different wt.% of NH<sub>4</sub>Br added polymer blend electrolytes. A broad and strong peak of hydroxyl group is present at 3287 cm<sup>-1</sup> and 3393 cm<sup>-1</sup> for cornstarch and PVP [22] respectively and this peak is shifted towards 3313 cm<sup>-1</sup> in 80 wt.% cornstarch and 20 wt.% PVP optimized polymer blend electrolyte. Similarly C–H stretching of cornstarch at 2927 cm<sup>-1</sup> is shifted slightly [23] for optimized polymer blend electrolyte system. The characteristics vibration bands of cornstarch: PVP blend system clearly depicts the presence of cornstarch and PVP. It is confirmed by presence of C–O stretching of cornstarch (1147, 995, and 929 cm<sup>-1</sup>) [24] and C=O stretching (1638 cm<sup>-1</sup>), CH<sub>2</sub> wagging (1437 cm<sup>-1</sup>), and C–N stretching (1292 cm<sup>-1</sup>) of optimized sample CPN-0

polymer blend electrolyte [25]. Furthermore, an addition of NH<sub>4</sub>Br salt in the optimized blend system modifies the peak intensity, peak shape, and position which reveals the occurrence of polymer-salt complex formation (Fig. 2b). The variations in peak position are clearly tabulated in Table 2. Suppression and broadening of C–H bands reveals the disturbance of the polymer chain arrangement due to the addition of salt and it also suggests the formation of complex. C=O stretching is shifted to 1639 cm<sup>-1</sup> in the polymer-salt complex system. It is the evidence of interaction between the salt and polymers not only rises from O–H group but also from C–O group [26, 27]. Within the tetrahedral H<sup>+</sup> ion, the bond with the N–H occurs in the structure of NH<sub>4</sub>Br. NH<sub>4</sub><sup>+</sup> directly towards the bromine ion (Br<sup>-</sup>), and thereby forms an N–H...Br hydrogen bond [28] via lone proton migration (H<sup>+</sup>) mechanism [29, 30]. Since loosely bounded H<sup>+</sup> in NH<sub>4</sub><sup>+</sup> ion is easily dissociated by the influence of dc electric field.

### FTIR deconvolution

The deconvolution technique is performed by using Origin 8 fitting software based on the Gaussian-Lorentz function used to perform. In the cornstarch, PVP:NH<sub>4</sub>Br polymer blend electrolytes attain C–O characterization peaks at 990 and 1045 cm<sup>-1</sup> [24]. The intensity of C–O peaks is varied, which reveals the presence of chemical reaction when different substances (inorganic salt and host polymer) are physically mixed. The deconvoluted FTIR spectrum of higher conducting polymer blend electrolyte is shown in Fig. 3. Intensity of those peaks is changed without change in wave-number. These modifications reflect the interactions among the polymer molecules [26]. The peak adjacent to 995 cm<sup>-1</sup> can be assigned to free ions and the peaks adjacent to 1036 cm<sup>-1</sup> and 1017 cm<sup>-1</sup> can be assigned to contact ions [31]. Percentage of free ions (%) can be calculated using

$$\text{Percentage of free ions (\%)} = \frac{A_f}{(A_f + A_c)} \times 100 \quad (1)$$

**Fig. 1** **a** XRD pattern of parent optimization and **b** different wt.% NH<sub>4</sub>Br added SPEs

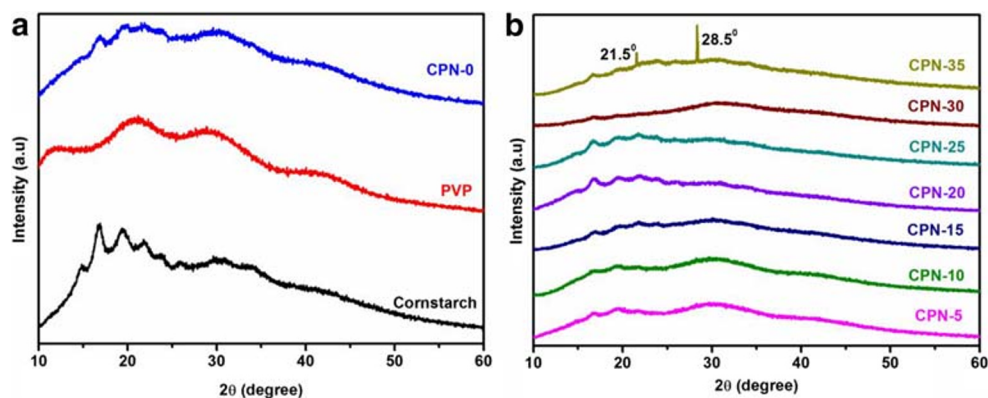


**Table 2** FTIR band assignment for prepared SPEs

Assignments	Wavenumber (cm <sup>-1</sup> )				
	Cornstarch	PVP	CPN-0	CPN-5	CPN-35
O–H stretching	3287	3393	3313	3301	3291
C–H stretching	2927	2951	2922	2928	2928
C=O stretching	-	1638	1655	1648	1639
CH <sub>2</sub> wagging	-	1437	1422	1428	1431
C–N stretching	-	1292	1288	1291	1291
C–O stretching of cornstarch	1147	-	1147	1149	1149
C–O in C–O–C of cornstarch	995	-	995	999	1003
C–O stretching of cornstarch	929	-	932	931	931

Here,  $A_f$  and  $A_c$  are the total area of free ion region and contact ion region respectively [32]. Table 3 lists the percentage of free ions and contact ions of prepared polymer electrolytes. The sample CPN-35 attains higher free ions than other composition. These free ions are the accountable for the ion conductivity in the polymer electrolytes.

## AC impedance analysis

### Nyquist plot

Nyquist plot of prepared SPEs is shown in Fig. 4a. Nyquist plot of CPN-0 polymer blend electrolyte illustrates a complete semicircle; it is due to the parallel combination of mobile and immobile charge carrier in the polymer chain [33]. For the samples CPN-0 to CPN-20, the Nyquist plot shows a semicircle at higher frequency with a spike at low frequency. The high frequency semicircle represents the bulk effect and the low frequency spike represents the polarization effect in the electrode-electrolyte interface [34]. For rest of the other compositions, the Nyquist plot has two semicircles with one spike. For the sample CPN-35, the impedance plot with two semicircles with spike is shown in Fig. 4b. The series of two parallel combinations of bulk resistance ( $R_b$ ) and bulk CPE with

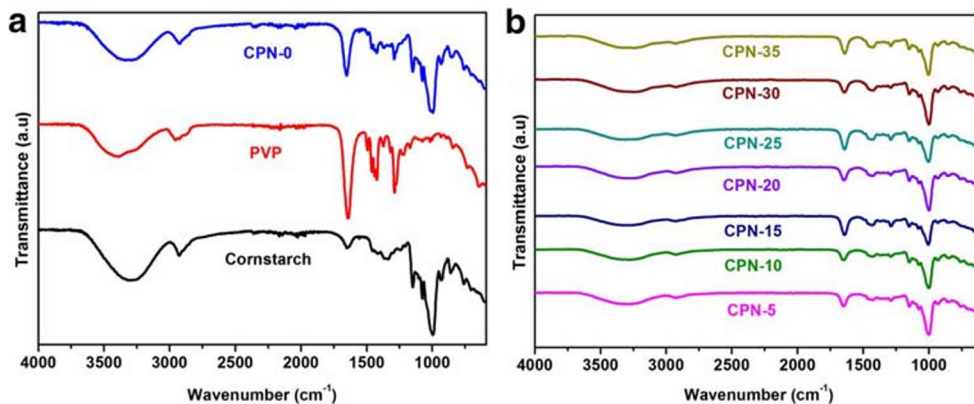
another CPE is an equivalent circuit for the samples CPN-25 to CPN-35. The two semicircles obtained for the above combinations are owing to the rise in the molecular packing between salt and blend polymer chain. These results indicate the enhanced reduction of resistance by improving amorphous behaviour in the composition.

Using the formula

$$\sigma = l/RbA \quad (2)$$

Conductivity of the sample is calculated. Here,  $l$  and  $A$  are the thickness and conduct area of the polymer membrane. The number of free ions migration in the polymer electrolyte is increased by addition of  $\text{NH}_4\text{Br}$  in the SPEs and thereby increases the conductivity [35]. Table 4 depicts the conductivity values of the prepared SPEs. For the sample CPN-30, the higher conductivity of  $3.14 \times 10^{-5} \text{ S cm}^{-1}$  and  $1.31 \times 10^{-4} \text{ S cm}^{-1}$  is obtained at 303 K and 358 K respectively. The value of the conductivity shows the increment three orders at higher composition. The amorphous nature is improved for higher conducting samples, which is verified from XRD pattern. The amorphous nature of the polymer can make the free space in the polymer chains to enhance the movement of ions. Furthermore, the higher composition sample has more protons

**Fig. 2** **a** FTIR spectrum for parent optimization and **b** different wt.%  $\text{NH}_4\text{Br}$  added SPEs



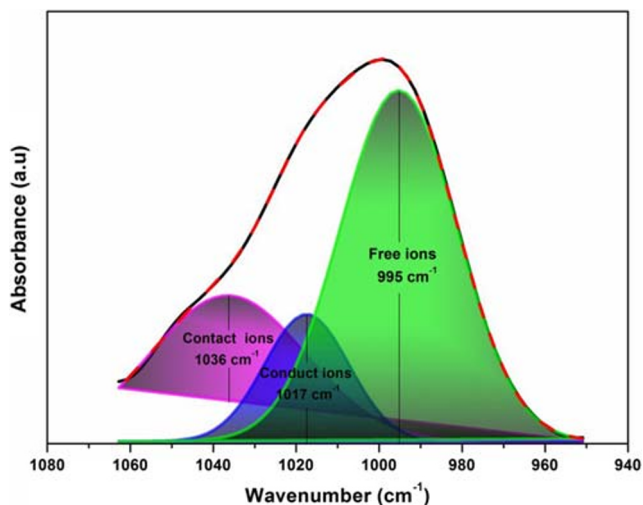


**Fig. 3** The deconvoluted FTIR spectrum of higher conducting polymer blend electrolyte

(H<sup>+</sup>) that are from the salt [36, 37]. Thus, the conductivity is abruptly increased and it is shown in different order in whole compositions. The conductivity is decreased to  $5.47 \times 10^{-5}$  S cm<sup>-1</sup> at 358 K due to the collision of ions [38].

**Investigation of conduction theory**

Figure 5 displays the frequency dependence conductance spectra of higher conducting electrolyte at different temperatures. This conductance spectrum is divided into three regions. In the region, I, the observed drop off conductivity is due to the space charge polarization/interfacial effect which acts on electrode and electrolyte surface at lower frequencies [39]. Plateau and dissipation regions [40] are overlapped in mid-frequency region II and higher frequency region III. In region II, the area of the overlapped dispersion region is higher than in region III. The high appearance of the plateau region may be occurred due to the form of more voids. It is the reason for the rapid ionic displacement of mobile charges in this region [41]. In region III, the area of the overlapped plateau region is greater than the plateau in the region II. The mobilization and

**Table 3** Percentage of free ions and conduct ions of the cornstarch/PVP/NH<sub>4</sub>Br SPEs

Sample	Free ions (%)	Conduct ions (%)
CPN-5	28.58	71.42
CPN-10	29.81	70.19
CPN-15	30.16	69.84
CPN-20	32.06	67.94
CPN-25	38.23	61.77
CPN-30	40.45	59.55
CPN-35	36.41	63.59

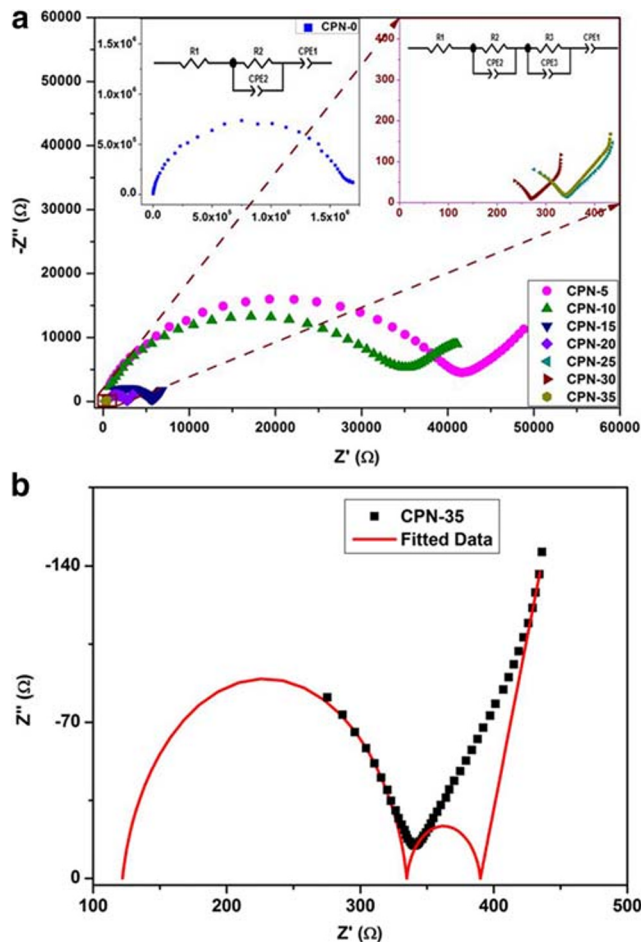


**Fig. 4** a Nyquist plot of prepared SPEs at 303 K b Nyquist plot of CPN-35 sample at 303 K

diffusion of mobile charges are having fewer enhancements at very high frequencies. When the temperature increases the conductivity also increases due to the elongation of free volume in the polymer matrix to enhance the conductivity as clearly visible in conductance spectra [42].

**Table 4** Activation energy and conductivity of the parent polymer blend and NH<sub>4</sub>Br added polymer blend electrolytes

Sample	E <sub>a</sub> (eV)	σ (S cm <sup>-1</sup> )	
		303 K	358 K
CPN-0	0.16	$5.24 \times 10^{-9}$	$1.16 \times 10^{-8}$
CPN-5	0.29	$1.94 \times 10^{-7}$	$1.06 \times 10^{-6}$
CPN-10	0.28	$2.35 \times 10^{-7}$	$1.31 \times 10^{-6}$
CPN-15	0.27	$1.55 \times 10^{-6}$	$9.29 \times 10^{-6}$
CPN-20	0.36	$3.46 \times 10^{-6}$	$2.43 \times 10^{-5}$
CPN-25	0.27	$2.42 \times 10^{-5}$	$1.25 \times 10^{-5}$
CPN-30	0.23	$3.14 \times 10^{-5}$	$1.31 \times 10^{-4}$
CPN-35	0.16	$1.89 \times 10^{-5}$	$4.48 \times 10^{-5}$

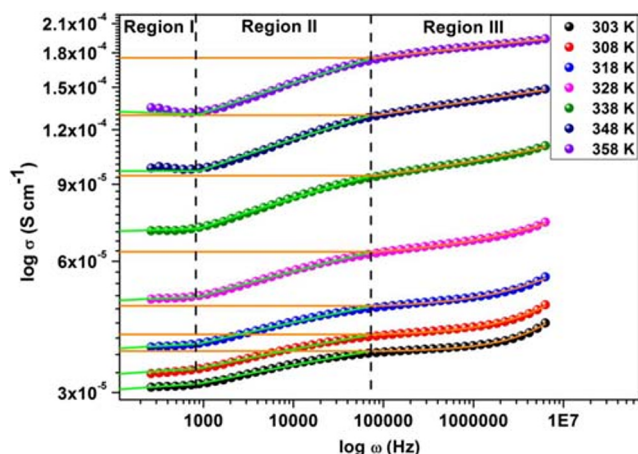


Fig. 5 Conduction spectra for higher conducting polymer blend electrolyte at different temperature

The universal power law is used to know about the ions dynamics of the polymer blend electrolyte

$$\sigma(\omega) = A\omega s + \sigma_{dc}, (0 < s < 1) \quad (3)$$

$$\text{Since, } \sigma_{ac} = A\omega^s$$

$$\log(\sigma - \sigma_{dc}) = \log A + \log \omega s \quad (4)$$

$$\log(\sigma - \sigma_{dc}) = \log A + s \log \omega \quad (5)$$

Here,  $s$  and  $A$  are the power law exponent value and temperature-dependent parameter. The exponent values of  $s_1$  and  $s_2$  are calculated from the non-linear fitting of conduction spectra with respect to region II and region III. The plot of exponent values ( $s_1$  and  $s_2$ ) versus temperature ( $T$ ) is shown in Fig. 6. Commonly, the exhibited polaron conduction obeys the following mechanisms [43–46]: correlated barrier hopping (CBH) model, quantum mechanical tunneling (QMT) model, overlapping large polaron tunneling (OLPT) model, and small polaron hopping (SPH) model.

The value of  $s_1$  is independent on temperature to follow the QMT model for conduction [47]. According to the quantum mechanical phenomenon, the polaron is formed by the combination of conducting proton and stress fields. The polarons travel through the potential barrier by the tunneling process. As explained in the QMT model, the AC conductivity is arising from electronic or atomic tunneling between equilibrium sites.

In high frequencies, when the temperature rises the value of  $s_2$  decreases. This implies that the conduction mechanism of the polymer electrolyte at high frequencies follows the OLPT [26]. This behaviour is attained due to the breaking of the internal connection between the sites and the relaxing ions. So the ions are not dependent with each other and stimulate the tunneling process than the hopping process.

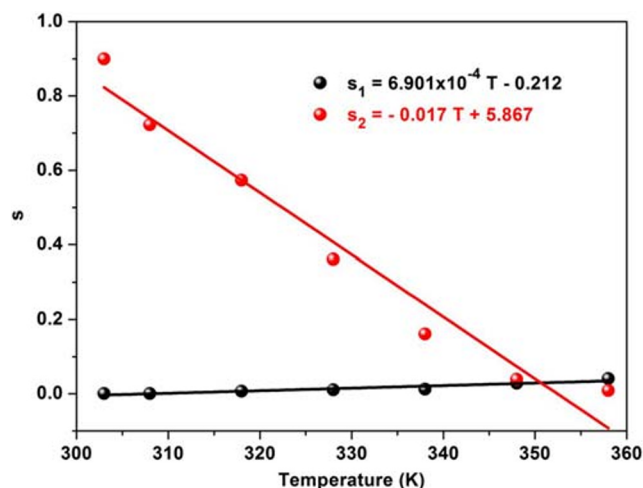


Fig. 6 The power law exponent value versus temperature

### Temperature-dependent conductivity/Arrhenius plot

Figure 7 displays the logarithm of conductivity versus temperature. The relationship between conductivity and Activation energy is described by Arrhenius model which is exposed in the equation,

$$\sigma T = \sigma_0 \exp\left(\frac{-E_a}{kT}\right) \quad (6)$$

By the concept of Arrhenius behaviour, the conductivities of all the prepared samples are linearly increased with temperature. The increment of ion dynamics in the polymer matrix is achieved by presence of free space segmental motion, local structural relaxation and hopping mechanism between the coordination sites [48]. Linear fit of this plot provides the slope value, it is used for calculate the activation energy of the samples are tabulated in Table 4. The activation energy is varied due to the necessity of energy of conductive ions

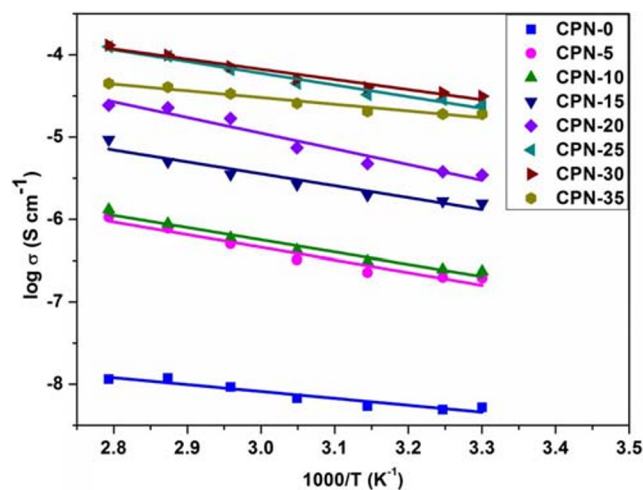


Fig. 7 Arrhenius plot of prepared SPEs

[49]. The obtained activation energy for the higher conducting sample (CPN-30) is 0.23 eV. The value of activation energy is little high for the highest conducting sample due to the energy requirement of conductive condition of ions [49] while increasing concentration, huge amount of the increments of charge carriers produced. Thus, the electrical conductivity is increased. Even though these ionic carriers occupy more space in the polymer chains, it can produce ion-ion interaction. Because of high movement with collision of other ions the polymer makes the best conductivity and little more activation energy.

**Dielectric studies**

Conductivity trend of polymer electrolytes and polarization effect in between electrode and electrolyte are stated by dielectric analysis. Charge storage and energy loss of polymer electrolytes are measured by dielectric constant ( $\epsilon'$ ) and dielectric loss ( $\epsilon''$ ) respectively. Figure 8a and b illustrate the dielectric constant and dielectric loss for prepared polymer blend electrolytes.  $\epsilon'$  and  $\epsilon''$  are calculated by the following equation [50, 51]. The calculated values of  $\epsilon'$  and  $\epsilon''$  are displayed in the Table 5.

$$\epsilon' = Z''/\omega C_0(Z'2 + Z''2) \tag{7}$$

and

$$\epsilon'' = Z'/\omega C_0(Z'2 + Z''2) \tag{8}$$

$\epsilon'$  and  $\epsilon''$  are reaching the higher value at lower frequency because of the space charge polarization at electrode|electrolyte interface, resulting a rise in the equivalent capacitance [52]. Due to the decrease of polarization effect,  $\epsilon'$  and  $\epsilon''$  are reduced by the applied higher frequency. This means that the prepared polymer blend electrolytes obey the non-Debye behaviour [53]. At higher frequency, there is no surplus ion diffusion present in the direction of the applied electrical field because of the existence of fast periodic reversal of the electric field [5]. The number of free ions or charge

carrier’s density is increased by the addition of salt in the polymer blend electrolyte. The maximum dielectric constant and dielectric loss are observed for the sample CPN-30. The same trend is revealed in the conductivity result.

**Modulus spectra analysis**

Figure 8c and d show the frequency dependence real ( $M'$ ) and imaginary ( $M''$ ) modulus spectra for prepared polymer blend electrolytes. The negligible contribution of electrode|electrolyte interface effect of both  $M'$  and  $M''$  are attained in the vicinity of zero at lower frequency. Appearance of long tail at lower frequency indicating the large capacitance related with the electrodes, thus indicates the non-Debye nature of prepared electrolytes [53]. At higher frequency, the values of both  $M'$  and  $M''$  are varied due to the attribution of bulk ionic movement of the materials [54]. While the salt concentration increases in the polymer blend electrolytes, the height of the hump is reduced. Due to the relaxation mechanism, the humps of both  $M'$  and  $M''$  are shifted towards the higher frequency.

**Dielectric energy dissipation factor**

Relaxation mechanism of prepared polymer blend electrolytes is investigated by dielectric energy dissipation factor ( $\tan \delta$ ) shown in Fig. 9. It denotes the ratio of the amount of energy lost to the amount of energy stored in a material [55].

$$\tan(\delta) = \left(\frac{\epsilon''}{\epsilon'}\right) \tag{9}$$

The hump of frequency dependence  $\tan \delta$  for different wt.%  $\text{NH}_4\text{Br}$  added polymer blend electrolytes are moved towards the higher frequency. The presence of shifting and height variations confirmed the non-Debye nature of samples. Occurrence of shifting is established due to the increment of charge carrier density and hence the faster the segmental relaxation in the samples by the addition of  $\text{NH}_4\text{Br}$  [56]. The relaxation time ( $\tau$ ) is measured by the reciprocal of corresponding frequency ( $\log \omega_{\max}$ ) of maximum height of the hump which is listed in Table 5. The conductivity relaxation is described by Kohlrausch-Williams-Watts (KWW) function  $\phi(t)$

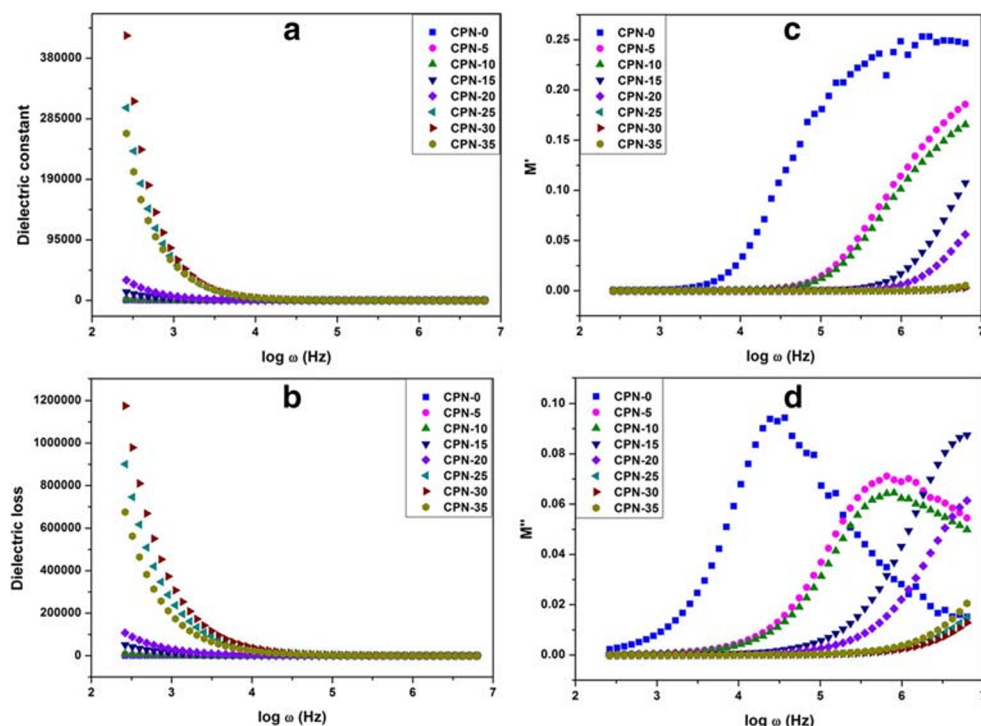
$$\phi(t) = \exp[-(t/\tau)^\beta] \tag{10}$$

Since  $\beta$  be the exponent parameter of Kohlrausch [57] and it is determined by  $\beta = 1.14/\text{FWHM}$ . Generally the obtained value of  $\beta$  is less than one ( $0 < \beta < 1$ ) and denotes the non-Debye model. The measured values are tabulated in Table 5. The higher conducting sample (CPN-30) attains higher  $\beta$  value (0.942).

**Table 5** Calculated value of relaxation time, FWHM, and  $\beta$

Composition	$\epsilon'$	$\epsilon''$	Relaxation time ( $\tau$ )	FWHM	$\beta$
CPN-0	4.07	1.55	$3.09 \times 10^{-3}$	1.948	0.585
CPN-5	19.95	24.59	$1.41 \times 10^{-4}$	1.997	0.721
CPN-10	43.10	36.81	$1.15 \times 10^{-4}$	1.994	0.722
CPN-15	87.38	46.36	$2.72 \times 10^{-5}$	1.977	0.728
CPN-20	203.71	101.15	$1.80 \times 10^{-5}$	1.563	0.921
CPN-25	414.44	365.27	$5.25 \times 10^{-6}$	1.560	0.923
CPN-30	449.56	394.78	$4.28 \times 10^{-6}$	1.529	0.942
CPN-35	224.78	198.78	$3.48 \times 10^{-6}$	1.549	0.930

**Fig. 8** **a** Dielectric constant, **b** dielectric loss, **c** real modulus, and **d** imaginary modulus of prepared SPEs



## Cyclic voltammetry

Electrochemical behaviour, redox process, stability of reaction products, and reversibility of a reaction of polymer electrolytes are studied with silver|electrolyte|silver configuration by cyclic voltammetry (CV). CV for the sample CPN-30 by changing the scan rate in the potential range of  $-0.4$  V to  $0.3$  V at ambient temperature is shown in Fig. 10. Oxidation and reduction peaks are observed in CV plot and it shows the pseudo capacitor behaviour [58]. The pseudo capacitor is a faradaic energy storage based on the fast redox reaction on near-surface region of the electrode [59]. The capacitive behaviour is also proved by the presence of linearly increasing

tilted spike at low frequency region in the Nyquist plot which is due to the ion adsorption occurrence at the electrode-electrolyte interface [40]. The redox peaks are increased due to the increase of scan rate. By expanding the scan rate, the ion movement is expanded because of the lessening in the resistance. Along these lines, the area of CV graph increases for the electrolyte. This is the confirmation of the proper interfacial compatibility and ionic and polaron conductions in the SPE [60]. In Fig. 10a and b shows the CV for first and twentieth cycle. Moreover, there is no change observed in oxidation, reduction and area from first to twentieth cycle. This behaviour confirms good electrochemical stability of the higher conducting polymer electrolyte [61].

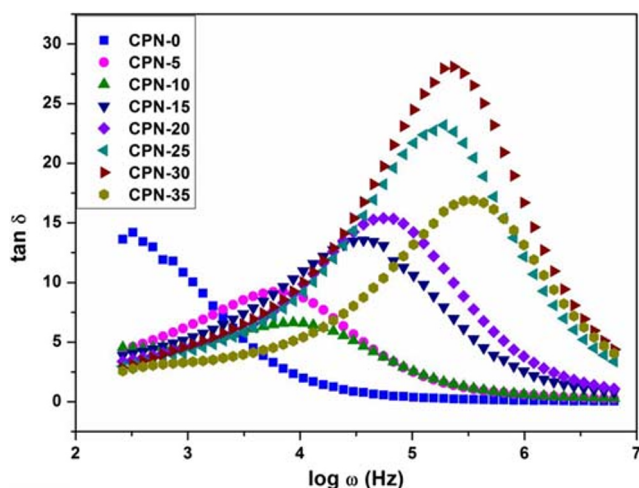


**Fig. 9** Variation of  $\tan \delta$  with frequency of prepared SPEs

## Ions transport study (Wagner's DC polarization technique)

Transport study is an utmost important study to relate the diffusion of ionic contribution in the electrolyte. In this Wagner's DC polarization technique, one graphite coated silver electrode (SEG) is used to restrict the flow of ions in the cell configuration of blocked SEG||SPE||SE. A constant potential of  $2$  V is applied to the polarized cell at room temperature. In the beginning, the high current is obtained due to transportation of ions and electrons. The SS electrodes prevent the flow of ions across the external circuit and this blockage of ions only permits the flow of electronic current. Then the current is rapidly decreased with time because of electrode polarization effect [49]. Now the flow of ions is restricted by blocked SEG. So the observed final saturated current ( $I_c$ ) is

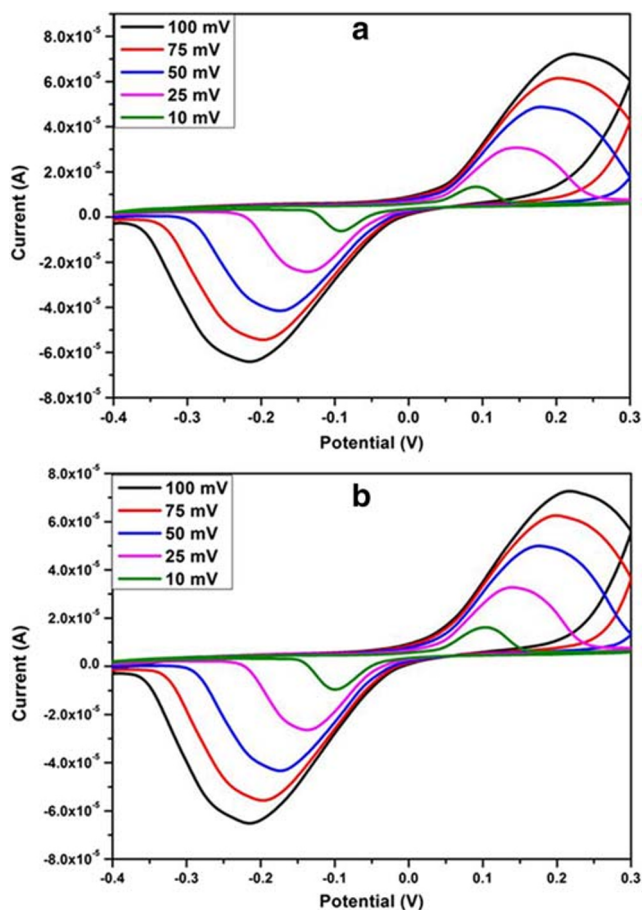


Fig. 10 a Cyclic voltammetry plot of higher conducting SPE by first cycle and b cyclic voltammetry plot of higher conducting SPE by 20th cycle

attributed only due to electron conduction in SPE [22, 49]. The distinction in current with a function of time is displayed in Fig. 11. The transference number of ions ( $t_{ion}$ ) and electron ( $t_{ele}$ ) are calculated by following relation

$$t_{ion} = \frac{I_t - I_c}{I_t} \text{ and } t_{ele} = 1 - t_{ion} \tag{11}$$

For all composition of polymer blend electrolytes, transference number is obtained as above 0.9. This is the confirmation of predominant ion conduction in cornstarch: PVP:NH<sub>4</sub>Br polymer blend electrolytes.

Number of charge carriers ( $n$ ), diffusion coefficients ( $D$ ), and mobility ( $\mu$ ) of cation and anion in polymer blend matrix is calculated by,

$$n = \frac{N\rho \times \text{molar ratio of salt}}{\text{molar weight of the salt}} \text{ (cm}^{-3}\text{)} \tag{12}$$

$$D = D_+ + D_- = \frac{KT\sigma}{ne^2} \text{ (cm}^2\text{/s)}, \quad t_{ion} = \frac{D_+}{D_+ + D_-} \text{ and } t_{ele} = \frac{D_-}{D_+ + D_-} \tag{13}$$

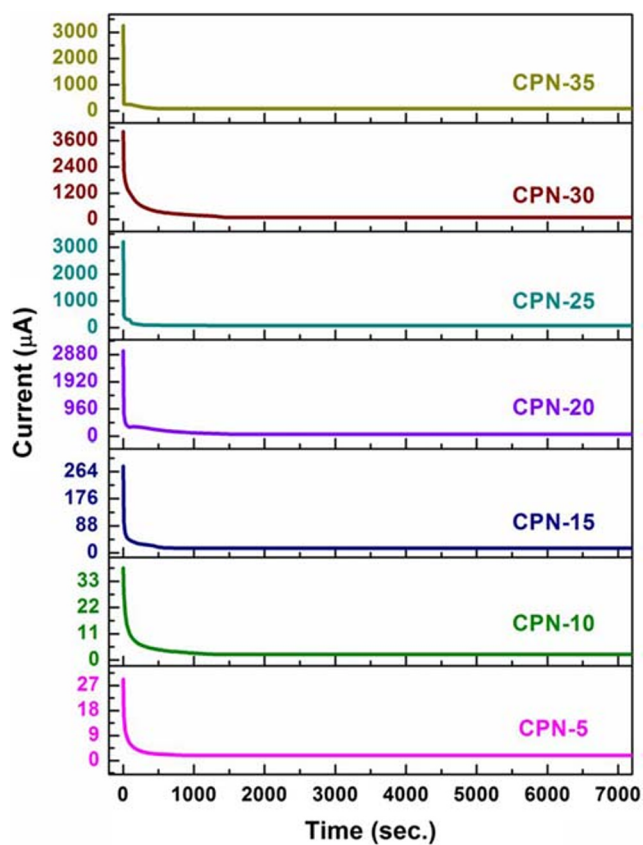


Fig. 11 Current versus time plots for NH<sub>4</sub>Br added polymer blend electrolytes

$$\mu = \mu_+ + \mu_- = \frac{\sigma}{ne} \text{ (cm}^2\text{/Vs)}, \quad t_{ion} = \frac{\mu_+}{\mu_+ + \mu_-} \text{ and } t_{ele} = \frac{\mu_-}{\mu_+ + \mu_-} \tag{14}$$

where

$N$  Avogadro’s number ( $6.023 \times 10^{23}$  particles per mole)

$\rho$  density of the salt (NH<sub>4</sub>Br = 2.429 g/cm<sup>3</sup>)

$K$  Boltzmann constant ( $1.3806 \times 10^{-23}$  m<sup>2</sup> kg s<sup>-2</sup> K<sup>-1</sup>)

$e$  charge of the electron ( $1.602 \times 10^{-19}$  C)

The transport parameters of prepared SPEs are listed in Table 6. The value of both diffusion coefficient ( $D$ ) and mobility ( $\mu$ ) are increased up to the sample CPN-30. The cation value of  $D$  and  $\mu$  is higher value than anion in all the polymer blend electrolytes. From this, it is concluded that  $D$  and  $\mu$  are responsible for the enhancement of ion conductivity in cornstarch:PVP:NH<sub>4</sub>Br polymer blend electrolytes.

### Electrochemical cell characterization

Electrochemical cell is prepared by graphite, anode (Zn + ZnSO<sub>4</sub>.7H<sub>2</sub>O), electrolyte (CPN-30), and cathode (MnO<sub>2</sub>).

**Table 6** Number of charge carrier concentration, transference numbers, diffusion coefficient, and mobility of NH<sub>4</sub>Br added polymer blend electrolytes

Molecular weight of salt in %	No. of charge carriers ( <i>n</i> ) in cm <sup>-3</sup> (× 10 <sup>21</sup> )	Transference number		Diffusion coefficient in cm <sup>2</sup> /s			Mobility ( <i>μ</i> ) in cm <sup>2</sup> /Vs		
		T <sub>ion</sub>	T <sub>ele</sub>	D	D+	D-	μ	μ+	μ-
0.05	0.75	0.93	0.07	3.83 × 10 <sup>-11</sup>	3.58 × 10 <sup>-11</sup>	2.49 × 10 <sup>-12</sup>	1.46 × 10 <sup>-9</sup>	1.37 × 10 <sup>-9</sup>	9.53 × 10 <sup>-11</sup>
0.1	1.49	0.94	0.06	2.31 × 10 <sup>-11</sup>	2.17 × 10 <sup>-11</sup>	1.44 × 10 <sup>-12</sup>	8.85 × 10 <sup>-10</sup>	8.30 × 10 <sup>-10</sup>	5.52 × 10 <sup>-11</sup>
0.15	2.24	0.95	0.05	9.25 × 10 <sup>-11</sup>	8.75 × 10 <sup>-11</sup>	5.03 × 10 <sup>-12</sup>	3.54 × 10 <sup>-9</sup>	3.35 × 10 <sup>-9</sup>	1.92 × 10 <sup>-10</sup>
0.2	2.99	0.97	0.03	1.42 × 10 <sup>-10</sup>	1.38 × 10 <sup>-10</sup>	3.59 × 10 <sup>-12</sup>	5.43 × 10 <sup>-9</sup>	5.30 × 10 <sup>-9</sup>	1.37 × 10 <sup>-10</sup>
0.25	3.73	0.97	0.03	9.28 × 10 <sup>-10</sup>	9.05 × 10 <sup>-10</sup>	2.28 × 10 <sup>-11</sup>	3.55 × 10 <sup>-8</sup>	3.46 × 10 <sup>-8</sup>	8.74 × 10 <sup>-10</sup>
0.3	4.48	0.98	0.02	9.67 × 10 <sup>-10</sup>	9.46 × 10 <sup>-10</sup>	2.13 × 10 <sup>-11</sup>	3.70 × 10 <sup>-8</sup>	3.62 × 10 <sup>-8</sup>	8.14 × 10 <sup>-10</sup>
0.35	5.22	0.97	0.03	6.66 × 10 <sup>-10</sup>	6.47 × 10 <sup>-10</sup>	1.86 × 10 <sup>-11</sup>	2.55 × 10 <sup>-8</sup>	2.47 × 10 <sup>-8</sup>	7.12 × 10 <sup>-10</sup>

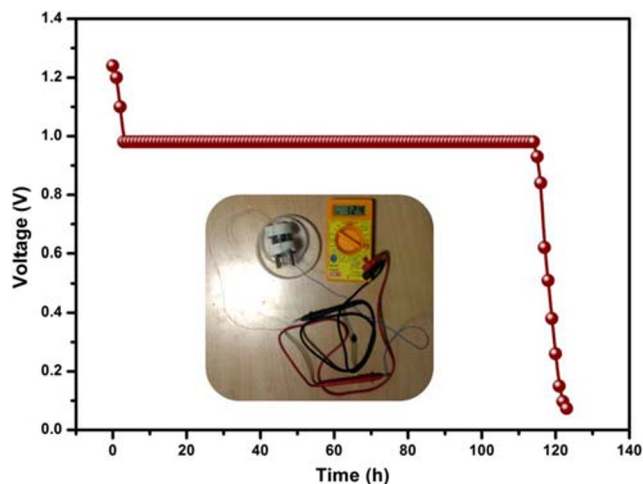
Open circuit voltage (OCV) of 1.24 V is obtained and displayed in Fig. 12. When the load (100KΩ) is connected across the cell, the short circuit current of 46 μA is observed and there is initial sharp continuous decrement in voltage is obtained for first 3 h because of active polarization. Because of the applying load, the discharging voltage decreased. The activation polarization is present when the rate of an electrochemical reaction at an electrode surface is controlled by sluggish electrode kinetics [62]. Battery discharge performance depends on the load. If there exists an increase in load (1Mohm resistance), the discharge time will be decreased [63]. The flow of charges is restricted by increase of load across the battery. In other hand energy density and discharge capacity also decreased. But power density of the battery does not affect by the variations in load. The voltage becomes stabilized at 0.98 V for 112 h. This constant voltage region is called as plateau region in discharge plot as shown in Fig. 12. After that region, the cell potential is decreased. Other cell parameters of the constructed proton conducting electrochemical cell are listed in Table 7.

**Table 7** Parameters of the electrochemical cell

OCV (V)	1.24
SCC (μA)	46
Area (cm <sup>2</sup> )	1.226
Weight (kg)	0.0027
Discharge time (h)	112
Current density (μA/cm <sup>2</sup> )	37.52
Power density (mW/Kg)	21.126
Energy density (mWh/Kg)	2366.104
Discharge capacity (μA/h)	0.411

## Conclusion

The various composition of NH<sub>4</sub>Br salt with Cornstarch: PVP polymer blend electrolyte was prepared by solution casting technique. Improvement of amorphous nature of polymer electrolyte by addition of NH<sub>4</sub>Br has confirmed by XRD. Moreover, all the analysis follows the same trend, is the best. The sample CPN-30 attains the conductivity value of 1.31 × 10<sup>-4</sup> S cm<sup>-1</sup> at 358 K. The conduction theory investigation obeys the QMT and OLPT conduction mechanism in mid-frequency region II and higher frequency region III respectively. The increment of ions in the blend polymers is also explicated in the studies of FTIR deconvolution technique and Wagner polarization methods. The Faradaic pseudo capacity behaviour of this higher conducting sample has observed from Cyclic Voltammetry study. A proton conducting

**Fig. 12** Photograph and discharge plot for constructed proton conducting electrochemical cell

electrochemical cell has prepared with the configuration of Graphite||Anode (Zn + ZnSO<sub>4</sub>·7H<sub>2</sub>O)||CPN-30||Cathode (MnO<sub>2</sub>)||Graphite and the measured open circuit potential is 1.24 V.

**Acknowledgments** The authors would like to thank Kalasalingam Academy of Research and Education for giving the technical and financial support.

## References

- Samsudin AS, Khairul WM, Isa MIN (2012) Characterization on the potential of carboxy methylcellulose for application as proton conducting biopolymer electrolytes. *J Non Cryst Solids*. 358:1104–1112. <https://doi.org/10.1016/j.jnoncrsol.2012.02.004>
- Li H, Tao Y, Zhang C, Liu D, Luo J, Fan W, Xu Y, Li Y, You C, Pan ZZ, Ye M, Chen Z, Dong Z, Wang DW, Kang F, Lu J, Yang QH (2018) Dense graphene monolith for high volumetric energy density Li–S batteries. *Adv Energy Mater*. 8. <https://doi.org/10.1002/aenm.201703438>
- Scrosati B (2000) Recent advances in lithium ion battery materials. *Electrochim Acta*. 45:2461–2466. [https://doi.org/10.1016/S0013-4686\(00\)00333-9](https://doi.org/10.1016/S0013-4686(00)00333-9)
- Zhu YS, Xiao SY, Li MX, Chang Z, Wang FX, Gao J, Wu YP (2015) Natural macromolecule based carboxymethyl cellulose as a gel polymer electrolyte with adjustable porosity for lithium ion batteries. *J Power Sources*. 288:368–375. <https://doi.org/10.1016/j.jpowsour.2015.04.117>
- Majid SR, Arof AK (2007) Electrical behavior of proton-conducting chitosan-phosphoric acid-based electrolytes. *Phys B Condens Matter*. 390:209–215. <https://doi.org/10.1016/j.physb.2006.08.038>
- Zhou G, Li F, Cheng HM (2014) Progress in flexible lithium batteries and future prospects. *Energy Environ Sci*
- Ren S, Zheng T, Zhou Q, Zhang L, Li H (2014) Preparation and ionic conductivity of composite polymer electrolytes based on hyperbranched star polymer. *Ionics (Kiel)*. 20:1225–1234. <https://doi.org/10.1007/s11581-013-1061-4>
- Sharma AL, Shukla N, Thakur AK (2008) Studies on structure property relationship in a polymer-clay nanocomposite film based on (pan)8LiClO<sub>4</sub>. *J Polym Sci Part B Polym Phys* 46:2577–2592. <https://doi.org/10.1002/polb.21583>
- Yoon MY, Hong SK, Hwang HJ (2013) Fabrication of Li-polymer/silica aerogel nanocomposite electrolyte for an all-solid-state lithium battery. *Ceram Int*. 39:9659–9663. <https://doi.org/10.1016/j.ceramint.2013.05.088>
- Di Noto V, Lavina S, Giffin GA, et al (2011) Polymer electrolytes: present, past and future. *Electrochim Acta*
- Yahya MZA, Arof AK (2004) Conductivity and X-ray photoelectron studies on lithium acetate doped chitosan films. *Carbohydr Polym*. 55:95–100. <https://doi.org/10.1016/j.carbpol.2003.08.018>
- Mohamed NS, Subban RHY, Arof AK (1995) Polymer batteries fabricated from lithium complexed acetylated chitosan. *J Power Sources*. 56:153–156. [https://doi.org/10.1016/0378-7753\(95\)80027-E](https://doi.org/10.1016/0378-7753(95)80027-E)
- Chandra S, Hashmi SA, Prasad G (1990) Studies on ammonium perchlorate doped polyethylene oxide polymer electrolyte. *Solid State Ionics*. 40–41:651–654. [https://doi.org/10.1016/0167-2738\(90\)90090-E](https://doi.org/10.1016/0167-2738(90)90090-E)
- Kumar M, Sekhon SS (2002) Ionic conductance behaviour of plasticized polymer electrolytes containing different plasticizers. *Ionics (Kiel)*. 8:223–233. <https://doi.org/10.1007/BF02376072>
- Karthikeyan S, Sikkanthar S, Selvasekarapandian S, Arunkumar D, Nithya H, Kawamura J (2016) Structural, electrical and electrochemical properties of polyacrylonitrile-ammonium hexafluorophosphate polymer electrolyte system. *J Polym Res*. 23. <https://doi.org/10.1007/s10965-016-0952-2>
- Sengwa RJ, Dhatarwal P, Choudhary S (2014) Role of preparation methods on the structural and dielectric properties of plasticized polymer blend electrolytes: correlation between ionic conductivity and dielectric parameters. *Electrochim Acta*. 142:359–370. <https://doi.org/10.1016/j.electacta.2014.07.120>
- Ramlli MA, Kamarudin KH, Isa MIN (2015) Ionic conductivity and structural analysis of carboxymethyl cellulose doped with ammonium fluoride as solid biopolymer electrolytes. *Am J Sustain Agric* 46+
- Shukur MF, Ithnin R, Kadir MFZ (2014) Electrical characterization of corn starch-LiOAc electrolytes and application in electrochemical double layer capacitor. *Electrochim Acta*. 136:204–216. <https://doi.org/10.1016/j.electacta.2014.05.075>
- Morita M, Araki F, Yoshimoto N et al (2000) Ionic conductance of polymeric electrolytes containing lithium salts mixed with rare earth salts. *Solid State Ionics*. 136–137:1167–1173. [https://doi.org/10.1016/S0167-2738\(00\)00613-5](https://doi.org/10.1016/S0167-2738(00)00613-5)
- Anjali Devi D, Smitha B, Sridhar S, Aminabhavi TM (2006) Novel crosslinked chitosan/poly(vinylpyrrolidone) blend membranes for dehydrating tetrahydrofuran by the pervaporation technique. *J Memb Sci*. 280:45–53. <https://doi.org/10.1016/j.memsci.2006.01.003>
- Hofmann A, Schulz M, Hanemann T (2013) Gel electrolytes based on ionic liquids for advanced lithium polymer batteries. *Electrochim Acta*. 89:823–831. <https://doi.org/10.1016/j.electacta.2012.10.144>
- Teoh KH, Lim CS, Ramesh S (2014) Lithium ion conduction in corn starch based solid polymer electrolytes. *Meas J Int Meas Confed*. 48:87–95. <https://doi.org/10.1016/j.measurement.2013.10.040>
- Mendes JF, Paschoalin RT, Carmona VB, Sena Neto AR, Marques ACP, Marconcini JM, Mattoso LHC, Medeiros ES, Oliveira JE (2016) Biodegradable polymer blends based on corn starch and thermoplastic chitosan processed by extrusion. *Carbohydr Polym*. 137:452–458. <https://doi.org/10.1016/j.carbpol.2015.10.093>
- Jinisha B, Anil Kumar KM, Manoj M et al (2017) Development of a novel type of solid polymer electrolyte for solid state lithium battery applications based on lithium enriched poly (ethylene oxide) (PEO)/poly (vinyl pyrrolidone) (PVP) blend polymer. *Electrochim Acta*. 235:210–222. <https://doi.org/10.1016/j.electacta.2017.03.118>
- Ramesh S, Liew CW, Arof AK (2011) Ion conducting corn starch biopolymer electrolytes doped with ionic liquid 1-butyl-3-methylimidazolium hexafluorophosphate. *J Non Cryst Solids*. 357:3654–3660. <https://doi.org/10.1016/j.jnoncrsol.2011.06.030>
- Yusof YM, Illias HA, Kadir MFZ (2014) Incorporation of NH<sub>4</sub>Br in PVA-chitosan blend-based polymer electrolyte and its effect on the conductivity and other electrical properties. *Ionics (Kiel)*. 20:1235–1245. <https://doi.org/10.1007/s11581-014-1096-1>
- Hema M, Selvasekarapandian S, Sakunthala A, Arunkumar D, Nithya H (2008) Structural, vibrational and electrical characterization of PVA-NH<sub>4</sub>Br polymer electrolyte system. *Phys B Condens*

- Matter. 403:2740–2747. <https://doi.org/10.1016/j.physb.2008.02.001>
28. Norby T (1999) Solid-state protonic conductors: principles, properties, progress and prospects. *Solid State Ionics*. 125:1–11. [https://doi.org/10.1016/S0167-2738\(99\)00152-6](https://doi.org/10.1016/S0167-2738(99)00152-6)
  29. Goodenough JB (1993) Proton conductors: solids, membranes, and gels-materials and devices. Edited by Phillippe Colomban, Cambridge University Press, Cambridge, UK 1992, £ 75, xxxii, 581 pp., hardcover, ISBN 0-521-38317-X. *Adv Mater*. <https://doi.org/10.1002/adma.19930050923>
  30. Vicentini NM, Dupuy N, Leitzelman M, Cereda MP, Sobral PJA (2005) Prediction of cassava starch edible film properties by chemometric analysis of infrared spectra. *Spectrosc Lett*. 38:749–767. <https://doi.org/10.1080/00387010500316080>
  31. Arof AK, Amirudin S, Yusof SZ, Noor IM (2014) A method based on impedance spectroscopy to determine transport properties of polymer electrolytes. *Phys Chem Chem Phys*. 16:1856–1867. <https://doi.org/10.1039/c3cp53830c>
  32. Malathi J, Kumaravadivel M, Brahmanandhan GM, Hema M, Baskaran R, Selvasekarapandian S (2010) Structural, thermal and electrical properties of PVA-LiCF<sub>3</sub>SO<sub>3</sub> polymer electrolyte. *J Non Cryst Solids*. 356:2277–2281. <https://doi.org/10.1016/j.jnoncrysol.2010.08.011>
  33. Karthikeyan A, Vinatier P, Levasseur A (2000) Study of lithium glassy solid electrolyte/electrode interface by impedance analysis. *Bull Mater Sci*. 23:179–183. <https://doi.org/10.1007/BF02719906>
  34. Mariappan CR, Govindaraj G (2002) Ac conductivity, dielectric studies and conductivity scaling of NASICON materials. *Mater Sci Eng B Solid-State Mater Adv Technol*. 94:82–88. [https://doi.org/10.1016/S0921-5107\(02\)00083-1](https://doi.org/10.1016/S0921-5107(02)00083-1)
  35. Muralidharan P, Venkateswarlu M, Satyanarayana N (2004) AC conductivity studies of lithium borosilicate glasses: synthesized by sol-gel process with various concentrations of nitric acid as a catalyst. *Mater Chem Phys*. 88:138–144. <https://doi.org/10.1016/j.matchemphys.2004.06.032>
  36. Samsudin AS, Lai HM, Isa MIN (2014) Biopolymer materials based carboxymethyl cellulose as a proton conducting biopolymer electrolyte for application in rechargeable proton battery. *ElectrochimicaActa*. 129:1–13. <https://doi.org/10.1016/j.electacta.2014.02.074>
  37. Zainuddin NK, Samsudin AS (2018) Investigation on the effect of NH<sub>4</sub>Br at transport properties in k-carrageenan based biopolymer electrolytes via structural and electrical analysis. *Materials Today Communications* 14:199–209. <https://doi.org/10.1016/j.mtcomm.2018.01.004>
  38. Winie T, Arof AK (2006) Transport properties of hexanoyl chitosan-based gel electrolyte. *Ionics (Kiel)*. 12:149–152. <https://doi.org/10.1007/s11581-006-0026-2>
  39. Buraidah MH, Teo LP, Majid SR, Arof AK (2009) Ionic conductivity by correlated barrier hopping in NH<sub>4</sub>I doped chitosan solid electrolyte. *Phys B Condens Matter*. 404:1373–1379. <https://doi.org/10.1016/j.physb.2008.12.027>
  40. Aziz SB (2016) Erratum to: Occurrence of electrical percolation threshold and observation of phase transition in chitosan(1-x): AgI<sub>x</sub>(0.05 ≤ x ≤ 0.2)-based ion-conducting solid polymer composites. *Appl Phys A* 122:785. <https://doi.org/10.1007/s00339-016-0272-8>
  41. Shukur MF, Ibrahim FM, Majid NA, Ithnin R, Kadir MFZ (2013) Electrical analysis of amorphous corn starch-based polymer electrolyte membranes doped with LiI. *Phys Scr*. 88:025601. <https://doi.org/10.1088/0031-8949/88/02/025601>
  42. Chai MN, Ramlli MA, Isa MIN (2013) Proton conductor of propylene carbonate-plasticized carboxyl methylcellulose-based solid polymer electrolyte. *Int J Polym Anal Charact*. 18:297–302. <https://doi.org/10.1080/1023666X.2013.784934>
  43. Isa MIN, Samsudin AS (2016) Potential study of biopolymer-based carboxymethylcellulose electrolytes system for solid-state battery application. *Int J Polym Mater Polym Biomater*. 65:561–567. <https://doi.org/10.1080/00914037.2016.1149844>
  44. Kufian MZ, Majid SR, Arof AK (2007) Dielectric and conduction mechanism studies of PVA-orthophosphoric acid polymer electrolyte. *Ionics (Kiel)*. 13:231–234. <https://doi.org/10.1007/s11581-007-0098-7>
  45. Sundaramahalingam K, Nallamuthu N, Manikandan A, Vanitha D, Muthuvinayagam M (2018) Studies on sodium nitrate based polyethylene oxide/polyvinyl pyrrolidone polymer blend electrolytes. *Phys B Condens Matter*. 547:55–63. <https://doi.org/10.1016/j.physb.2018.08.002>
  46. Duraikkan V, Sultan AB, Nallaperumal N, Shunmuganarayanan A (2018) Structural, thermal and electrical properties of polyvinyl alcohol/poly(vinyl pyrrolidone)-sodium nitrate solid polymer blend electrolyte. *Ionics (Kiel)*. 24:139–151. <https://doi.org/10.1007/s11581-017-2169-8>
  47. Pradhan DK, Choudhary RNP, Samantaray BK (2008) Studies of structural, thermal and electrical behavior of polymer nanocomposite electrolytes. *Express Polym Lett*. 2:630–638. <https://doi.org/10.3144/expresspolymlett.2008.76>
  48. Mishra R, Rao KJ (1998) Electrical conductivity studies of poly(ethyleneoxide)-poly(vinylalcohol) blends. *Solid State Ionics*. 106:113–127. [https://doi.org/10.1016/s0167-2738\(97\)00493-1](https://doi.org/10.1016/s0167-2738(97)00493-1)
  49. Tu Z, Yu K, Lu Y, Archer LA (2014) Nanoporous polymer ceramic composite electrolytes for lithium metal batteries. *Adv Energy Mater* 4. <https://doi.org/10.1002/aenm.201300654>
  50. Mishra R, Baskaran N, Ramakrishnan PA, Rao KJ (1998) Lithium ion conduction in extreme polymer in salt regime. *Solid State Ionics*. 112:261–273. [https://doi.org/10.1016/s0167-2738\(98\)00209-4](https://doi.org/10.1016/s0167-2738(98)00209-4)
  51. Baskaran R, Selvasekarapandian S, Kuwata N, Kawamura J, Hattori T (2006) AC impedance, DSC and FT-IR investigations on (x)PVAc-(1-x)PVdF blends with LiClO<sub>4</sub>. *Mater Chem Phys*. 98:55–61. <https://doi.org/10.1016/j.matchemphys.2005.08.063>
  52. Ahmed HT, Abdullah OG (2019) Preparation and composition optimization of PEO: MC polymer blend films to enhance electrical conductivity. *Polymers (Basel)*. 11. <https://doi.org/10.3390/polym11050853>
  53. Zhou W, Kou Y, Yuan M, Li B, Cai H, Li Z, Chen F, Liu X, Wang G, Chen Q, Dang ZM (2019) Polymer composites filled with core@double-shell structured fillers: effects of multiple shells on dielectric and thermal properties. *Compos Sci Technol*. 181:107686. <https://doi.org/10.1016/j.compscitech.2019.107686>
  54. Hashmi SA, Kumar A, Tripathi SK (2007) Experimental studies on poly methyl methacrylate based gel polymer electrolytes for application in electrical double layer capacitors. *J Phys D Appl Phys*. 40:6527–6534. <https://doi.org/10.1088/0022-3727/40/21/010>
  55. Subba Reddy CV, Sharma AK, Narasimha Rao VVR (2003) Conductivity and discharge characteristics of polyblend (PVP + PVA + KIO<sub>3</sub>) electrolyte. *J Power Sources*. 114:338–345. [https://doi.org/10.1016/S0378-7753\(02\)00582-7](https://doi.org/10.1016/S0378-7753(02)00582-7)
  56. Shukur MF, Ithnin R, Kadir MFZ (2014) Electrical properties of proton conducting solid biopolymer electrolytes based on starch-chitosan blend. *Ionics (Kiel)*. 20:977–999. <https://doi.org/10.1007/s11581-013-1033-8>
  57. Teo LP, Buraidah MH, Nor AFM, Majid SR (2012) Conductivity and dielectric studies of Li<sub>2</sub>SnO<sub>3</sub>. *Ionics (Kiel)*. 18:655–665. <https://doi.org/10.1007/s11581-012-0667-2>
  58. Buraidah MH, Arof AK (2011) Characterization of chitosan/PVA blended electrolyte doped with NH<sub>4</sub>I. *J Non Cryst Solids*. 357:3261–3266. <https://doi.org/10.1016/j.jnoncrysol.2011.05.021>
  59. Arof AK, Kadir MFZ, Majid SR (2010) Plasticized chitosan-PVA blend polymer electrolyte based proton battery. *Electrochim Acta*

60. Conway BE, Pell WG (2003) Double-layer and pseudocapacitance types of electrochemical capacitors and their applications to the development of hybrid devices. *J Solid State Electrochem.* 7:637–644. <https://doi.org/10.1007/s10008-003-0395-7>
61. Balo L, Shalu GH, Kumar Singh V, Kumar Singh R (2017) Flexible gel polymer electrolyte based on ionic liquid EMIMTFSI for rechargeable battery application. *Electrochim Acta.* 230:123–131. <https://doi.org/10.1016/j.electacta.2017.01.177>
62. Broadhead J, Kuo HC (2001) Electrochemical principles and reactions. In: Linden D, Reddy TB (eds) *Handbook of batteries*, 3rd edn. McGraw-Hill, New York
63. Premalatha M, Vijaya N, Selvasekarapandian S, Selvalakshmi S (2016) Characterization of blend polymer PVA-PVP complexed with ammonium thiocyanate. *Ionics.* 22:1299–1310. <https://doi.org/10.1007/s11581-016-1672-7>

**Publisher's note** Springer Nature remains neutral with regard to jurisdictional claims in published maps and institutional affiliations.